The American Journal of
PATHOLOGY

ajp.amjpathol.org

ANIMAL MODELS

A Spontaneous Deletion within the Desmoglein 3 Extracellular Domain of Mice Results in Hypomorphic Protein Expression, Immunodeficiency, and a Wasting Disease Phenotype

Evgueni I. Kountikov,* Jonathan C. Poe,* Nancie J. MacIver,[†] Jeffrey C. Rathmell,[‡] and Thomas F. Tedder*

From the Departments of Immunology,* Pediatrics,[†] and Pharmacology and Cancer Biology,[‡] Duke University Medical Center, Durham, North Carolina

Desmoglein 3 is a transmembrane component of desmosome complexes that mediate epidermal cell-to-cell adhesion and tissue integrity. Antibody blockade of desmoglein 3 function in pemphigus vulgaris patients leads to skin blistering (acantholysis) and oral mucosa lesions. Desmoglein 3 deficiency in mice leads to a phenotype characterized by cyclic alopecia in addition to the dramatic skin and mucocutaneous acantholysis observed in pemphigus patients. In this study, mice that developed an overt squeaky (*sqk*) phenotype were identified with obstructed airways, cyclic hair loss, and severe immunodeficiency subsequent to the development of oral lesions and malnutrition. Single-nucleotide polymorphism—based quantitative trait loci mapping revealed a genetic deletion that resulted in expression of a hypomorphic desmoglein 3 protein with a truncation of an extracellular cadherin domain. Because hypomorphic expression of a truncated desmoglein 3 protein led to a spectrum of severe pathology not observed in mice deficient in desmoglein 3, similar human genetic alterations may also disrupt desmosome function and induce a disease course distinct from pathogenesis of pemphigus vulgaris. *(Am J Pathol 2015, 185: 617—630; http://dx.doi.org/10.1016/j.ajpath.2014.10.025)*

Tissues experiencing mechanical stress are held together by supramolecular desmosome complexes composed of type I transmembrane glycoproteins from the desmoglein (Dsg) and desmocollin (Dsc) families of epithelial cadherins.[1] The extracellular protein domains of the desmogleins and desmocollins consist of four approximately 110—amino acid homologous cadherin domains (EC1 to EC4) and a proximal extracellular anchor domain. The desmosomal cadherins are differentially expressed in different cellular layers of select tissues. For example, desmoglein 1 (Dsg1) is expressed at high levels in the suprabasal outer layer of skin epidermis (stratified squamous epithelia) and thymus.[2,3] Desmoglein 2 (Dsg2) is expressed ubiquitously in the basal layers of the epidermis and desmosome-enriched cardiac tissues.[2,3] Desmoglein 3 (Dsg3) is primarily expressed by epidermal keratinocytes in the basal and immediate suprabasal layers of skin and in the basal layer of the mucosal epithelium of the mouth, eyes, and trachea.[2,3] Six *Dsg* and three *Dsc* genes are found in mice, with four *Dsg* and three *Dsc* genes in humans.[4]

Homophilic and heterophilic interactions between the Dsg and Dsc proteins lead to the formation of tightly packed desmosomal complexes.[5]

The desmogleins are involved in human disease pathogenesis. Cleavage of the extracellular domain of Dsg1 by *Staphylococcus aureus* exfoliating toxin results in bullous impetigo in children, manifesting as skin blisters due to detachment (acantholysis) of the outer layer of epidermis.[6] Inactivation of either the *Dsg2* or *Dsc3* gene is embryonic lethal.[7,8] The development of circulating IgG autoantibodies against Dsg1 or Dsg3 can result in the human autoimmune blistering disorders pemphigus foliaceus and pemphigus vulgaris due to reduced desmoglein expression on the cell surface.[9] In patients with pemphigus foliaceus, acantholysis within the superficial layers of the epidermis results in clinical lesions that resemble those observed in lupus

erythematosus and seborrheic dermatitis patients. Pemphigus foliaceus patients experience no oral involvement and have no associated mortality. By contrast, patients with pemphigus vulgaris experience acantholysis within the deep basilar and parabasilar portions of the epidermis, which results in lesions that may resemble toxic epidermal necrolysis. With pemphigus vulgaris, there is significant oral and skin involvement and untreated patients experience considerable mortality.

Although mutations in the human *Dsg3* gene have not been described, gene inactivation in $Dsg3^{-/-}$ mice leads to fragility of the skin and oral mucous membranes, analogous to those found in pemphigus vulgaris patients,[10] along with runting and progressive hair loss.[11] Two independent spontaneous mutations within mouse chromosome 18 affecting exons encoding the Dsg3 cytoplasmic domain also ablate protein expression and lead to a $Dsg3^{-/-}$ phenotype.[10,12,13] Herein, a spontaneous gene mutation was identified in mice that develop an overt squeaky (*sqk*) phenotype with cyclic hair loss, obstructed airways, and severe immunodeficiency subsequent to the development of oral lesions and malnutrition. This phenotype was mapped to a partial exon deletion in the *Dsg3* gene that results in hypomorphic expression of a truncated Dsg3 protein, which leads to a severe spectrum of pathology not observed in $Dsg3^{-/-}$ mice.

Materials and Methods

Mouse SNP Genotyping and QTL Analysis

C57BL/6 (B6) and 129S1 (129) mice (The Jackson Laboratories, Bar Harbor, ME) were maintained in specific pathogen-free housing. Vanilla-flavored Ensure Plus nutrition shake (Abbott Laboratories, Abbott Park, RI) was used to supplement solid food for select experiments. Mice were euthanized if a predetermined level of distress was reached before natural death. All procedures were approved by the Duke University (Durham, NC) Institutional Animal Care and Use Committee.

B6 mice with the *sqk* phenotype were crossed with 129 wild-type (WT) mice to generate heterozygous F_1 progeny. The F_1 mice were intercrossed using sister-brother mating pairs to produce F_2 progeny, which were monitored for emergence of the *sqk* phenotype after the age of 3 weeks. Purified genomic DNA from tail snips of 74 F_2 mice was used for genome-wide genotyping of 222 single-nucleotide polymorphism (SNPs) that are distinct between the B6 and 129 mouse genomes. Genotyping (Duke University Genotyping Facility) used an Illumina BeadArray platform (Illumina, San Diego, CA). Quantitative trait loci (QTL) mapping was performed by calculating logarithm of odds (LOD) scores for each SNP using permutation test and J-QTL regression analysis software version 1.3.3 (The Jackson Laboratories). TaqMan PCR probes for amplifying SNPs flanking the region with a high LOD score were selected

using SNPBrowser software version 2.0 (Applied Biosystems, Carlsbad, CA). The probes were used to identify crossovers among 510 F_2 mouse DNA samples using an ABI 7900HT PRC machine and SDS software version 2.3 (Applied Biosystems). Additional internal SNPs for fine mapping were identified using the SNP database dbSNP build 138 (Short Genetic Variations, http://www.ncbi.nlm.nih.gov/projects/SNP, last accessed October 23, 2014) and Mouse Genome Informatics (Mouse SNP Query Form, http://www.informatics.jax.org/javawi2/servlet/WIFetch?page=snpQF, last accessed October 23, 2014) databases. The genotype of each SNP was determined after amplicon sequencing (Duke Cancer Center DNA Analysis Facility) as single-nucleotide (homozygous B6:B6) or double-nucleotide (heterozygous B6:129) peaks.

Immunofluorescence Staining and Analysis

Immunofluorescence staining was as described.[14] The following antibodies (Abs) were used: fluorescein isothiocyanate−, phosphatidylethanolamine-, phosphatidylethanolamine-cyanine 7−, or allophycocyanin-conjugated monoclonal Abs to mouse CD93 (clone AA4.1), B220 (30-F11), CD4 (RM4-5), and CD8 (53-6.7) (BioLegend, San Diego, CA); and anti-IgM Ab (goat; Southern Biotech, Birmingham, AL). Single-cell splenocytes and thymocytes were prepared by macerating spleens or thymuses between frosted ends of glass slides (Gold Seal; VWR International, Radnor, PA). Bone marrow cells were flushed from femurs and resuspended in phosphate-buffered saline. Cells were washed with phosphate-buffered saline containing 1% fetal bovine serum. Red blood cells were removed by lysis before single-cell leukocyte suspensions (10^6 cells) were stained at 4°C using predetermined optimal concentrations of fluorochrome-conjugated Abs for 20 minutes. Multicolor immunofluorescence analysis of cell surface molecule expression used a BD FACSCanto II (BD Biosciences, Franklin Lakes, NJ). Background staining levels were determined using nonreactive isotype-matched, fluorochrome-conjugated control monoclonal Abs (BioLegend and Southern Biotech).

PCR Analysis

Total RNA was extracted from tissues using TRIzol reagent (Life Technologies, Carlsbad, CA), according to the manufacturer's instructions. cDNA was synthesized from sample RNA using random or oligo-d(T)$_{25}$ primers and SuperScript III Reverse Transcriptase (Life Technologies), according to the manufacturer's protocols. Primer pairs that generated overlapping 500- to 800-bp amplicons were used to amplify the entire coding sequence of *Dsg3* transcripts. Sequencing revealed a deletion within Dsg3$^{sqk/sqk}$ cDNAs that were amplified using the following primers: 5′-TACCTACCG-CATTTCTGGAGTG-3′ (forward) and 5′-TCCAGAGCC-TTAACCACCTTC-3′ (reverse). Genomic DNAs flanking this deletion were amplified and sequenced using flanking
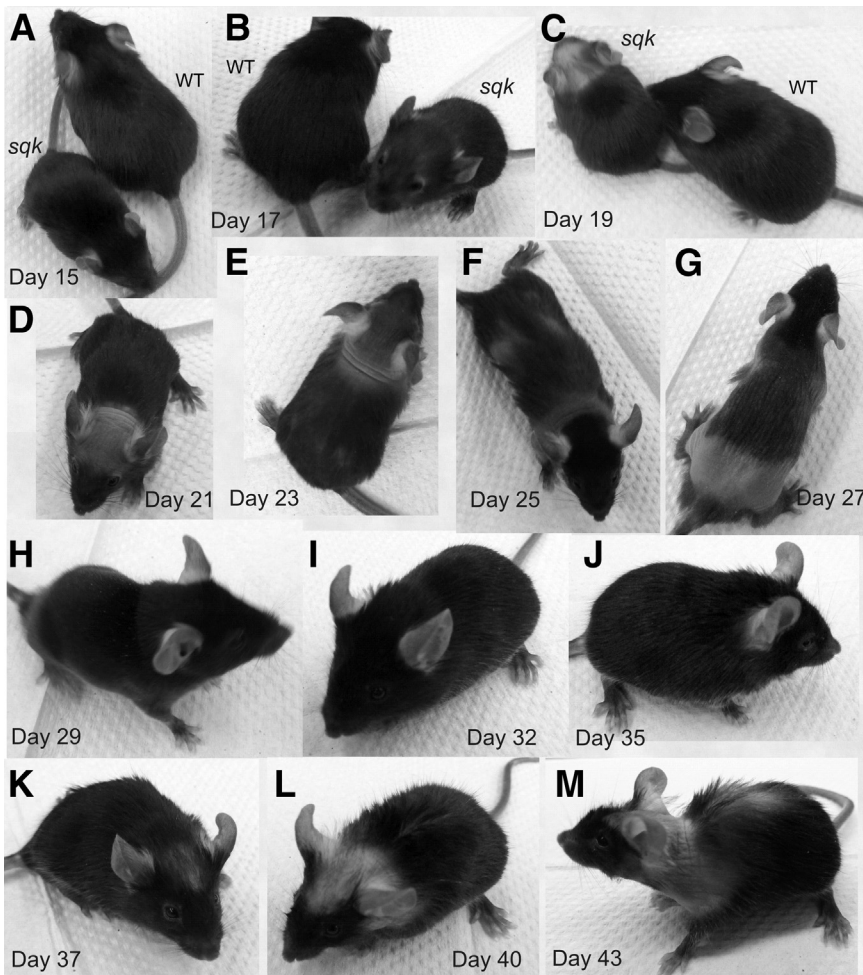
Figure 1 Runting and time course of cyclic hair loss in squeaky (*sqk*) mice. Images of *sqk* and wild-type (WT) littermates were taken every 2 to 3 days starting at day 15 after birth. **A–C:** Although no visible differences between the mice are observed before day 12, *sqk* mice are identifiable thereafter by diminished size (runting), when compared to WT littermates (days 15 to 19). **B–G:** By days 17 to 18, *sqk* mice develop a thinning of the hair coat characterized by a bald spot on the head, which then progresses from head to tail by day 25 to 27. **E–H:** New hair growth becomes evident on the head area where hair loss was first observed (eg, from days 23 to 27), which then progresses from head to tail in a pattern similar to the hair loss. **I** and **J:** The *sqk* mice (32 to 35 days old) recover nearly normal hair coats. **K–M:** A second, less synchronized, hair loss cycle begins on days 36 to 38.

primers: 5′-GGCACTGGCATCACCTCA-3′ (forward) and 5′-AGCACTGGGAAGTTGTCATTG-3′ (reverse).

For real-time PCR quantification, cDNA synthesized using random primers from equal amounts of total RNA was analyzed using a Eppendorf Mastercycle Instrument (Eppendorf, Hamburg, Germany), SYBR Fast real-time quantitative PCR kits (KAPA Biosystems, Woburn, MA), and Dsg3-specific primers: 5′-CCAGACACACCAGCAACAATG-3′ (forward) and 5′-CAGCAGCACCACCATCAGG-3′ (reverse). 18S RNA-specific primers [5′-AGTGAAACTGCGAATGGC-3′ (forward) and 5′-CCGTCGGCATGTATTAGC-3′ (reverse)] were used for normalization. Relative Dsg3 mRNA expression was quantified as described,[15] using the REST program (REST version 2, *http://rest-2009.gene-quantification.info*, last accessed October 23, 2014).

Histological and Protein Expression Analysis

For immunofluorescence staining of frozen tissue sections, the samples were fixed in methanol at −20°C, prepared as described,[16] and stained using a mouse monoclonal Ab specific for desmoplakin or anti-plakoglobin polyclonal rabbit Ab (both generously provided by Dr. Terry Lechler, Duke University,

Durham, NC). Alternatively, tissues were fixed in 10% formalin and embedded in paraffin. Six 5-um–thick tissue sections were stained with hematoxylin and eosin.

Tongue or skin specimens (approximately 10 μg) from 3-day-old *Dsg3^{sqk/sqk}*, *Dsg3^{sqk/+}*, and *Dsg3^{+/+}* littermates were homogenized and solubilized in 140 μL of reducing SDS sample buffer containing 1 μL protein inhibitor cocktail (Set III; Thermo Fisher Scientific, Waltham, MA), as described.[17] Samples were boiled for 8 minutes before insoluble materials were removed by centrifugation for 10 minutes at $13,000 \times g$ at 4°C. Tongue (10 μL) and skin (6 μL) sample supernatant fluid was resolved by 4% to 12% SDS-PAGE (Life Technologies), transferred to nitrocellulose membranes in 10 mmol/L *N*-cyclohexyl-3-amino-propanesulfonic acid buffer (pH 10.4), and blocked with a 3% solution of dry fat-free milk in washing buffer (50 mmol/L Tris-HCl, 150 mmol/L NaCl, and 0.05% Tween-20, pH 7.5). Blocked membranes were first incubated with a 1:1000 dilution of M-20 goat polyclonal Ab (Santa Cruz Biotech, Dallas, TX) reactive with the C-terminus of the mouse Dsg3 protein, washed, and then incubated with horseradish peroxidase–conjugated donkey anti-goat IgG (heavy and light chains) secondary Ab (Jackson
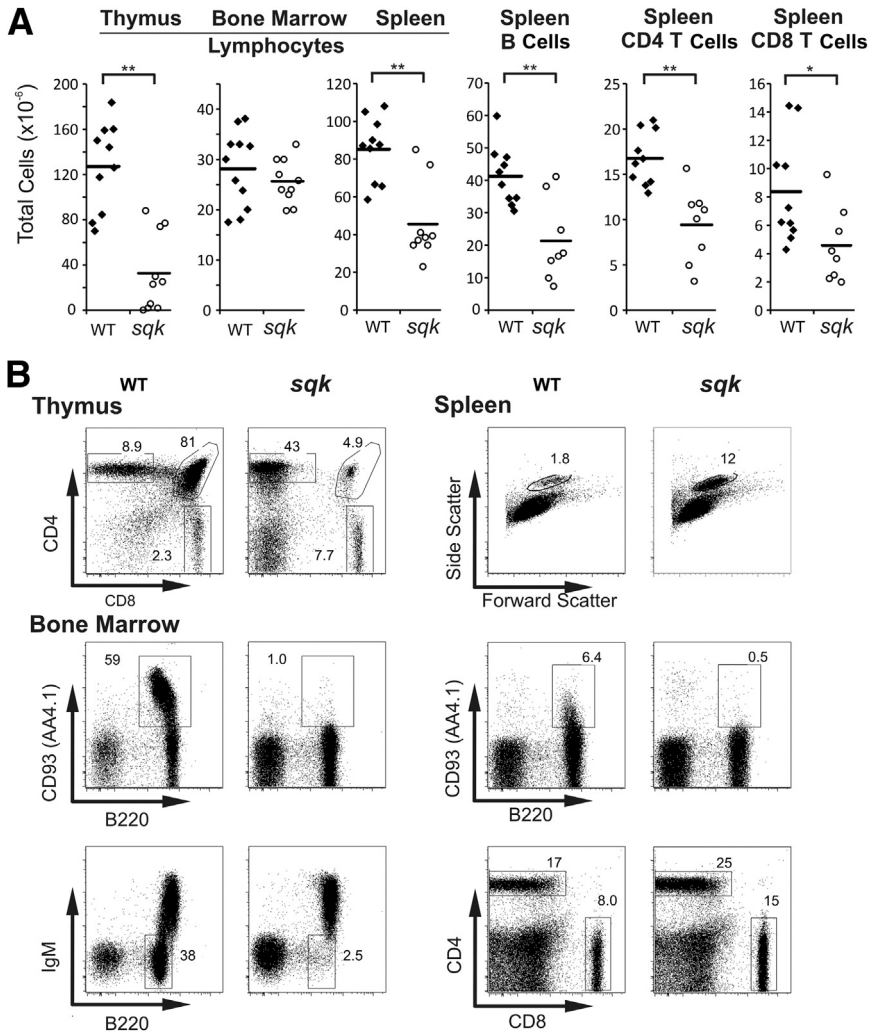
Figure 2 Deficient T- and B-lymphocyte development in squeaky (*sqk*) mice. **A:** Lymphocyte numbers within the thymus, bone marrow (single femur), and spleen of wild-type (WT; black diamonds) and *sqk* (white circles) mice. Each symbol is an individual mouse. Bars indicate means with statistical significance determined using a one-tailed paired Student's *t*-test. Age-matched WT and *sqk* mouse pairs were between 4 and 24 weeks of age. **B:** Immunofluorescence staining of leukocytes harvested from the thymus, bone marrow, and spleen of representative *sqk* and WT littermates at 14 weeks of age with flow cytometry analysis. Numbers indicate representative percentages of cells within the indicated gates. The gates define double-positive (CD4$^+$CD8$^+$) and single-positive (CD4$^-$CD8$^+$ or CD4$^+$CD8$^-$) thymocytes; pre- and immature (CD93$^+$B220^{low}) B cells and pre-B (B220^{low}IgM$^-$) cells in bone marrow; and spleen large granular cells with high side scatter (eg, neutrophils), transitional B cells (CD93$^+$B220$^+$), and T-cell subsets. Similar results were obtained from four or more mice of each genotype. *$P < 0.05$, **$P < 0.01$.

ImmunoResearch, West Grove, PA) diluted at 1:25,000 in washing buffer. Dsg3-specific bands were visualized using a Pico Chemiluminescence Kit (Thermo Fisher Scientific) with exposure to autoradiography film (Kodak, Rochester, NY). Equivalent protein loading between the samples was confirmed using ERK2-specific primary Ab at a 1:1,500 dilution (Santa Cruz Biotech) and horseradish peroxidase—conjugated donkey anti-rabbit IgG (heavy and light chain) secondary Ab at a 1:25,000 dilution (Jackson Immuno-Research) after the membrane was stripped and reblocked as described.[17]

Primary mouse epidermal keratinocytes were derived as described.[18] Intracellular keratinocyte adhesion was measured as described.[19,20] Western blot analysis was performed as described above using Ab specific to Dsc1, Dsc3 (R&D Systems, Minneapolis, MN), desmoplakin, and plakoglobin (provided by Dr. Terry Lechler, Duke University) at dilutions 1:5000, 1:2000, 1:1400, and 1:700, respectively.

Serum leptin concentrations were measured by enzyme-linked immunosorbent assays using Leptin Mouse Quantikine enzyme-linked immunosorbent assay kits (R&D Systems), as per the manufacturer's instructions.

Statistical Analysis

The two-tailed Student's *t*-test was used for statistical analysis. Error bars were calculated as SEM. $P < 0.05$ was considered significant. Statistical significance for differences in real-time PCR results was calculated using REST 2009 software version 1. Differences in body weight were evaluated using analysis of covariance and RStudio software version 0.98.1091 (RStudio, Boston, MA).

Results

Identification of the *sqk* Phenotype

Three B6 littermates in our breeding colony were visually identified to have a runted appearance with significant hair loss. This phenotype was not transmitted directly to offspring, but runting and hair loss reappeared when brother-sister offspring were interbred. In addition, breathing was labored in runted adult mice with hair loss, which was accompanied by a distinct squeaking sound (Supplemental Video S1). This squeaky (*sqk*$^{+/+}$) phenotype

A Breeding Strategy

B QTL Linkage Analysis
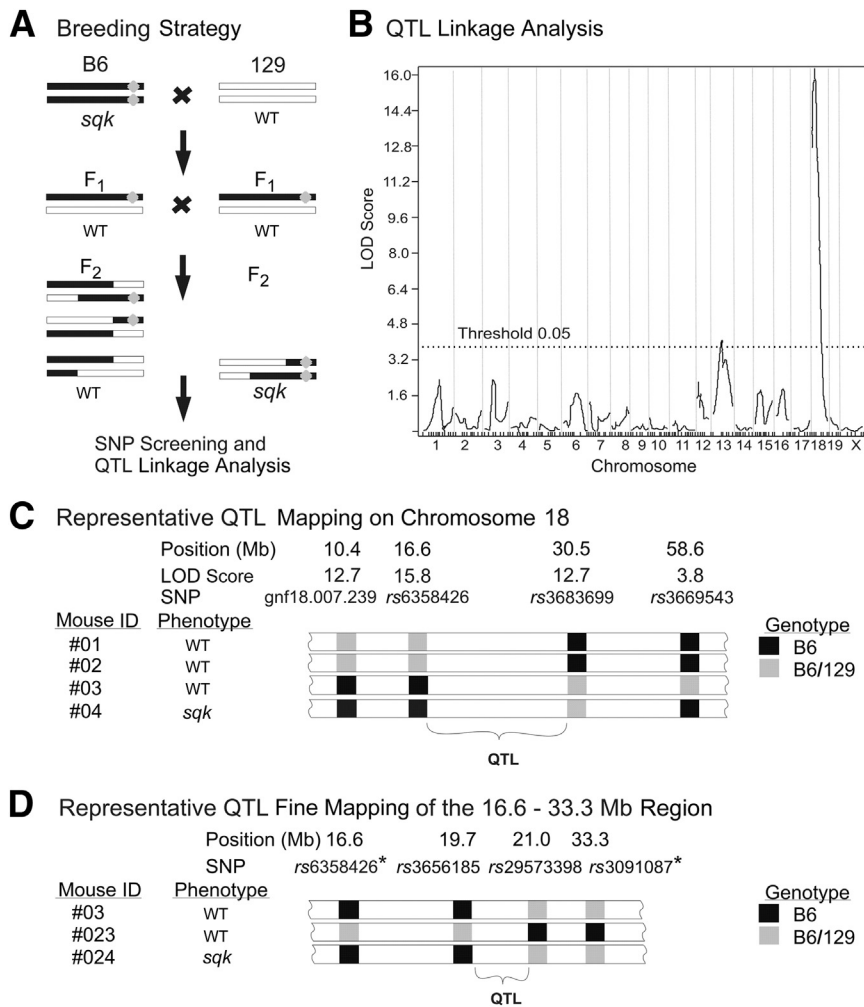
Figure 3 Genomic mapping of the squeaky (*sqk*) mutation. **A:** Breeding strategy for genome-wide quantitative trait loci (QTL) analysis. The *sqk* mice [C57BL/6 (B6) genetic background] were bred with wild-type (WT) 129S1 (129) mice. F_1 offspring heterozygous *B6/129* at all chromosome locations were subsequently intercrossed to produce F_2 mice. F_2 mice had independent chromosomal assortment and crossovers, with 25% of the F_2 mice displaying the *sqk* phenotype due to homozygosity of the responsible B6 genetic locus. **B:** The genomic locus responsible for the *sqk* phenotype maps to the proximal end of chromosome 18. High logarithm of odds (LOD) scores for three consecutive single-nucleotide polymorphisms (SNPs) indicate a high probability of association. SNP locations are indicated by the small vertical marks on the x axis. The vertical grid lines separate chromosomes. The threshold (dashed) line indicates a confidence level of 0.05. **C:** The phenotype and respective SNP genotype of four mice with crossovers most proximate to the QTL of interest, as identified in Supplemental Figure S1A. The 16.6- to 30.5-Mbp QTL location identified by mouse phenotype and genotype is shown. **D:** Fine mapping of the *sqk* QTL within the interval identified in **C** using three F_2 mice with informative crossovers, as identified in Supplemental Figure S1B. **Asterisks** indicate locations of TaqMan probes used to screen samples for fine mapping.

C Representative QTL Mapping on Chromosome 18

D Representative QTL Fine Mapping of the 16.6 - 33.3 Mb Region

was inherited in a mendelian manner with a recessive trait frequency of approximately 25%. Female *sqk* mice were unable to maintain viable litters. Therefore, male $sqk^{+/+}$ mice were bred with WT female mice, followed by brother-sister pairing of their offspring to generate mice for these studies.

Although $sqk^{+/+}$ neonates were indistinguishable from their littermates, their growth rates began to lag at the age of 12 to 14 days. By the age of 17 to 18 days, affected mice were easily identified by thinning of the hair coat beginning on the head, which then progressed from the head to the tail with a complete or nearly complete loss of hair (Figure 1). Hair loss occurred in a cyclical pattern, with regrowth visible by day 21, which was followed by the same pattern of head-to-tail hair loss. The subsequent loss of regrown hair was apparent by day 36, but the cycle of hair loss and regrowth was less synchronized, which resulted in older *sqk* mice having a patchy appearance with disparate-sized bald spots in their fur at random locations. Death rates of $sqk^{+/+}$ mice increased beginning at 2 weeks of age and resulted, in part, from infections that were usually characterized by conjunctivitis and bloated intestines.

Adult *sqk* Mice Develop Immunodeficiency

The reduced viability of adult *sqk* mice was associated with acquired immunodeficiency. T- and B-cell development was equivalent in 2- to 3-week-old WT mice and $sqk^{+/+}$ mice without obvious signs of runting or disease (data not shown). Thereafter, thymic cellularity was markedly reduced in *sqk* mice (Figure 2A), with a dramatic reduction in $CD4^+CD8^+$ double-positive thymocytes relative to WT littermates (Figure 2B). There was also a dramatic reduction in IgM^-B220^+ pre-B and $CD93^+$ immature B cells in the bone marrow and a reduction of $CD93^+$ immature/transitional B cells in the spleen. Although mature spleen T- and B-cell frequencies were not impaired in *sqk* mice relative to their WT littermates, total lymphocyte numbers were markedly reduced (Figure 2A). The frequency of splenic neutrophils with high forward and side light scatter properties was also significantly increased ($P < 0.05$, $n = 4$) in adult *sqk* mice (Figure 2B).

QTL Mapping of the *sqk* Mutation

For QTL mapping of the genetic alteration responsible for the *sqk* phenotype, the mutation was treated as a *B6*

Table 1 Genes within the Chromosome 18 Region Containing the *sqk* QTL

Start (bp)	Stop (bp)	Gene symbol	Description
19960930	20002097	*Dsc3*	Desmocollin 3
20030798	20059505	*Dsc2*	Desmocollin 2
20084703	20114773	*Dsc1*	Desmocollin 1
20247340	20283923	*Dsg1c*	Desmoglein 1 γ
20310873	20343353	*Dsg1a*	Desmoglein 1 α
20376835	20409741	*Dsg1b*	Desmoglein 1 β
20436175	20471821	*Dsg4*	Desmoglein 4
20498392	20509806	*Gm5688*	Tubulin, α 1C pseudogene/predicted gene 5688
20510304	20541310	*Dsg3*	Desmoglein 3
20548028	20549358	*Tpi-rs10*	Triosephosphate isomerase—related sequence 10
20558116	20604526	*Dsg2*	Desmoglein 2
20665250	20674326	*Ttr*	Transthyretin
20682557	20683002	*Gm10269*	Ribosomal protein L35 pseudogene/predicted gene 10269
20684599	20746404	*B4galt6*	UDP-Gal:βGlcNAc β-1,4-galactosyltransferase 6
20817224	20896078	*Trappc8*	Trafficking protein particle complex 8
20944625	20983848	*Rnf125*	Ring finger protein 125

QTL, quantitative trait loci; *sqk*, squeaky.

germline-specific allele. The *sqk* mice were crossed with WT 129 strain mice (Figure 3A). F_1 offspring were thus heterozygous *B6/129* for all genetic loci and did not exhibit the *sqk* phenotype. F_1 mice were subsequently intercrossed in brother-sister pairs to generate genetically distinct F_2 littermates due to independent chromosomal assortment and crossovers during gametogenesis. As expected for a recessive trait, approximately 23% of 74 F_2 mice exhibited the *sqk* phenotype, as monitored by runting and cyclic hair loss. Therefore, the *sqk* phenotype required homozygosity at a critical locus.

A forward genetic linkage analysis was used to identify the genomic element associated with the *sqk* phenotype. By using genomic DNA from 74 F_2 mice, 17 of which had the *sqk* phenotype, genome-wide genotyping of 222 informative SNPs between the B6 and 129 mouse strains was performed. QTL mapping revealed a single genetic locus with high LOD scores (12.7 to 15.8) on the proximal end of chromosome 18 (Figure 3B). LOD score is a measure of association between an observed trait and a specific SNP genotype. The SNP with the highest LOD score (15.8) was positioned at 16.6 Mbp, and was flanked by SNPs at 10.4 and 30.5 Mbp that each gave LOD scores of 12.7 (Figure 3C). A minor peak with a LOD score above the statistical threshold for significance was observed within chromosome 13 (Figure 3B). However, this region was excluded from consideration because analysis of the contributing SNP genotypes indicated a preponderance of 129-specific SNPs, whereas the *sqk* QTL was associated with a B6 genotype.

Twenty-two mice were identified with crossovers within the proximal portion of chromosome 18 (Supplemental Figure S1A). Four mice had particularly informative adjacent crossovers within the high LOD score region of interest (Figure 3C). On the basis of the association of the *sqk* phenotype with the B6 genotype, the QTL of interest was located between the two SNPs located at 16.6 and 30.5 Mbp. The QTL is upstream of the 30.5-Mbp SNP in WT

mouse 01, whereas WT mouse 03 demonstrated that the QTL was downstream of the 16.6-Mbp SNP. This interval was mapped further using 38 additional F_2 *sqk* and WT mice with crossovers between the 16.6- and 33.3-Mbp SNPs identified using flanking TaqMan probes (Figure 3D and Supplemental Figure S1B). The analysis of 14 additional SNPs by dye termination sequencing localized the *sqk* locus to a 1.3-Mbp region on chromosome 18 between SNPs at 19.7 and 21.0 Mbp. Probabilities for multiple mutations in the identified locus were calculated using spontaneous mutation rate estimates and the Poisson distribution.[21,22] The probability of a single germline point mutation per 1.3-Mbp region would be 2.9×10^{-3} mutations per year or 1 mutation per 350 mouse years. The probability of two or three point mutations within this locus would be 4.1×10^{-6} or 3.9×10^{-9} mutations per year, respectively. Therefore, this study focused on identifying single mutations within the identified locus.

Identification of the Gene Harboring the *sqk* Mutation

The refined *sqk* locus housed 16 genes (Table 1), including all six desmoglein and all three desmocollin genes. Remarkably, the *sqk* phenotype resembled mice with the bal and pas spontaneous mutations within their *Dsg3* genes.[12,23] Cyclic hair loss and skin lesions also characterize *Dsg3*-deficient mice.[10,11] Therefore, Dsg3 cDNA generated from tongue and the *Dsg3* gene from *sqk* mice were probed for length alterations using PCR primer sets. Indeed, nucleotide sequence analysis of products from two PCR primer pairs mapped a 1092-bp deletion in the *Dsg3* gene of *sqk* mice to a region between the 3' end of intron 5 and a part of exon 7 (Figure 4, A and B). This deletion resulted in the complete loss of exon 6 and 12 codons of exon 7. Despite this, the resulting cDNA splice variant of *Dsg3* remained in frame due to exon 5 splicing to a cryptic splice acceptor site within exon 7. The predicted polypeptide resulting from this
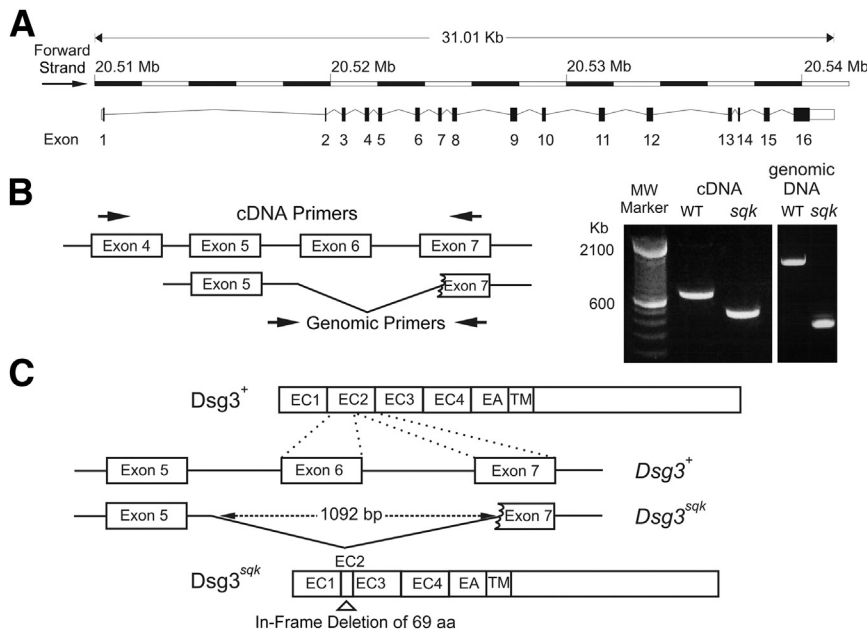
Figure 4 A desmoglein 3 (*Dsg3*) gene segment deletion in squeaky (*sqk*) mice. **A:** *Dsg3* gene organization in wild-type (WT) mice. A ruler indicates the gene position on chromosome 18, with each horizontal bar equal to 2 Kbp. The *Dsg3*^{+} gene contains 16 exons depicted as vertical bars connected with a thin line representing intronic regions. The **white boxes** at exons 1 and 16 are the 5' and 3' untranslated regions, respectively. **B:** A mapped deletion within the *Dsg3*[sqk] gene, as detected by PCR amplification of cDNA and genomic DNA. Diagram on the left indicates the locations of the primers (**arrows**) used for PCR analysis. The PCR-amplified cDNA and genomic DNA fragments were analyzed on the basis of size, as shown at the right. **C:** Comparison of *Dsg3*^{+} and *Dsg3*[sqk] gene fragments and the protein sequences they encode (Dsg3^{+} and Dsg3[sqk]). The 1092-bp *Dsg3*[sqk] gene deletion spanning intron 5 and part of exon 7 results in an in-frame deletion of 69 predicted amino acids (aa) within the extracellular cadherin domain 2 (EC2) of the translated protein.

genetic deletion and subsequent splicing event had a loss of 69 amino acids within the EC2 domain (Figure 4C), one of the four EC domains of Dsg3 that together are responsible for its Ca^{2+}-dependent adhesive function.[1] For the remainder of this article, *sqk* mice are referred to as *Dsg3*[sqk/sqk], their genotyped WT littermates as *Dsg3*^{+/+}, and their genotyped heterozygous littermates as *Dsg3*[sqk/+].

Because the *Dsg3*[sqk] deletion resulted in the synthesis of an in-frame Dsg3 protein variant, expression was verified using both real-time quantitative PCR and Western blot analyses. Real-time quantitative PCR analysis of cDNA from *Dsg3*[sqk/sqk], *Dsg3*[sqk/+], and *Dsg3*^{+/+} mice was performed using a forward primer specific to the 5' end of exon 1 and a reverse primer spanning the splice junction between exons 1 and 2 (Figure 5A). *Dsg3* transcript levels were similar between all three genotypes, indicating that *Dsg3* transcription and mRNA stability were not affected by the genomic deletion. For Western blot analysis, proteins extracted from whole skin and tongue were resolved by SDS-PAGE, transferred to nitrocellulose membrane, and probed with a Dsg3-specific polyclonal antibody. A faint Dsg3 protein band of reduced size was present in both the tongue and skin samples of both *Dsg3*[sqk/sqk] and *Dsg3*[sqk/+] mice (Figure 5B). In *Dsg3*[sqk/+] mice, the hypomorphic Dsg3 protein band was much fainter than the WT protein band in both *Dsg3*[sqk/+] and *Dsg3*^{+/+} mice. Equivalent total protein loading between samples was verified using a polyclonal antibody specific for ERK2 protein. Considering similar *Dsg3* transcript levels between genotypes (Figure 5A), these data indicate that Dsg3[sqk] protein was expressed, but at low levels, relative to native protein.

Hypomorphic Dsg3[sqk] expression and disrupted desmosome assembly may affect tissue resistance to mechanical stress.[19,20] Therefore, keratinocytes were purified from the skin of WT and *Dsg3*[sqk/sqk] neonatal mice and grown as confluent cell monolayers. Keratinocyte differentiation and up-regulated expression of desmosome proteins were induced by calcium. Mechanical stress induced by shaking the cell monolayers resulted in approximately 80% increase in the numbers of monolayer fragments from *Dsg3*[sqk/sqk] littermates when compared with cells from littermates with WT phenotype (Figure 5C). Keratinocytes from *Dsg3*[sqk/sqk] and *Dsg3*[sqk/+] mice also expressed significantly reduced levels of Dsg3[sqk] and Dsc3, whereas Dsc1 and placoglobin expression levels were not measurably altered (Figure 5D).

Tissue Pathology in *Dsg3*[sqk] Mice

Hair loss from most areas of the skin and the unique squeaking sound of *Dsg3*[sqk/sqk] mice suggest potential defects in epidermal and epithelial tissues and restricted airways. The impact of the *Dsg3*[sqk] mutation was, therefore, assessed on tissues that normally express abundant quantities of Dsg3. The thickness of pseudostratified ciliated epithelium in cross sections of trachea from *Dsg3*[sqk/sqk] mice was markedly increased (Figure 6A). Further examination of the upper respiratory pathways and larynx revealed a significant hyperplasia of the epiglottis resulting in its deformation and thickening, which visibly obstructed the airway (Figure 6, B and C). Histological staining of larynx sagittal sections revealed a subglottic stenosis and cartilage deformities (Figure 6D). The thickness of epithelial layers in the laryngeal areas, especially the stratum spinosum, was abnormally increased, which severely obstructed the airway (Figure 6, E and F). Snout tissue cross sections from *Dsg3*[sqk/sqk] mice also showed evidence of inflammation and thickening of the epidermis, particularly of the stratum spinosum (Figure 6G). Some *Dsg3*[sqk/sqk] mice also

A

qPCR Primers
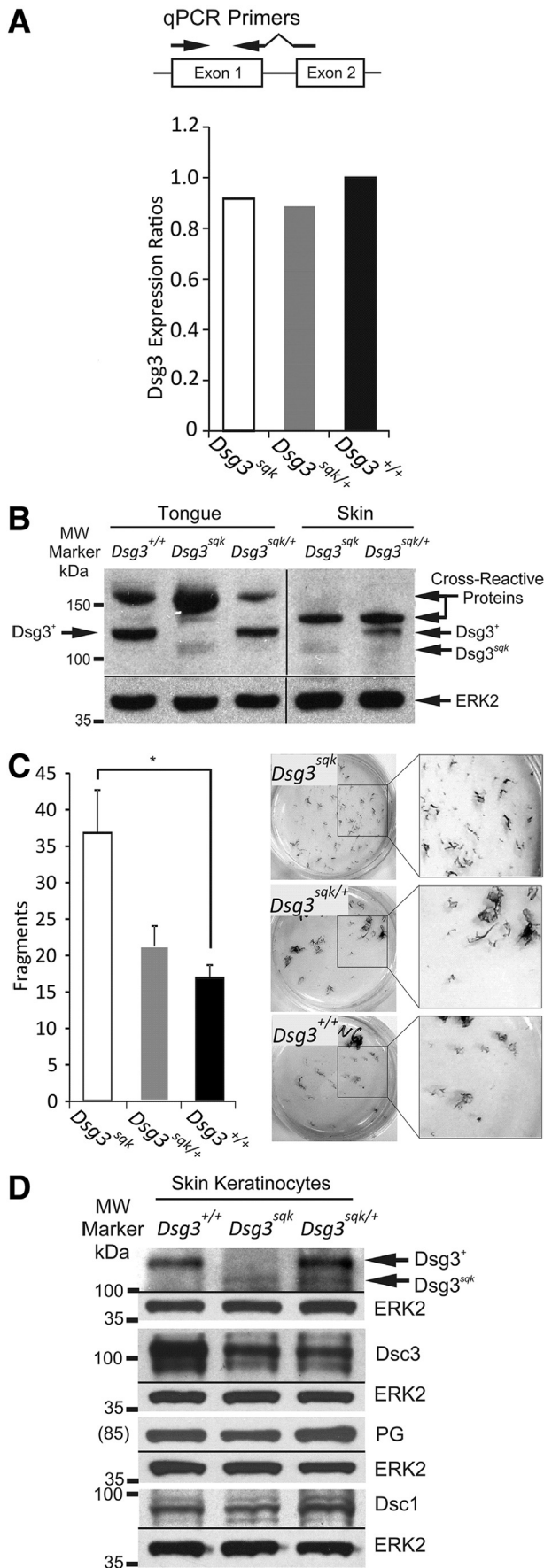
developed erosions of the snout, possibly due to the impaired healing of abrasions. Thickening of the epidermis and obstructed upper airways were in accord with the observed inspiratory stridor (squeaking) of $Dsg3^{sqk/sqk}$ mice.

The expression of desmosome structural components other than Dsg3 was studied by immunofluorescence staining of tongue sections, where Dsg3 is highly expressed. Desmoplakin and desmoglobin staining within tissues were both reduced in $Dsg3^{sqk/sqk}$ mice (Figure 6, H−J). Tongue lesions with a loss of suprabasilar epithelium were also observed in $Dsg3^{sqk/sqk}$ mice (Figure 6K), but the colon and the large and small intestines were normal (data not shown). $Dsg3^{sqk/sqk}$ mice also developed oral lesions similar to those described in $Dsg3^{-/-}$ mice and in humans with pemphigus vulgaris.[10] However, no evidence for acantholysis or separation of the suprabasilar epithelium was observed in $Dsg3^{sqk/sqk}$ mice.

$Dsg3^{sqk/sqk}$ Mice Exhibit a Starvation Phenotype

Despite their normal size during early life, $Dsg3^{sqk/sqk}$ mice become notably emaciated with age when compared to $Dsg3^{sqk/+}$ and $Dsg3^{+/+}$ littermates (Figure 7, A and B). Approximately 2% of $Dsg3^{sqk/sqk}$ mice also developed dorsa-ventral rib cage flattening (Figure 7C). Serum levels of leptin, an adipose-derived hormone, were also significantly reduced in $Dsg3^{sqk/sqk}$ mice (Figure 7D). Accordingly, $Dsg3^{sqk/sqk}$ mice had reduced body fat. As an example, the skin s.c. fat layer of $Dsg3^{sqk/sqk}$ mice was dramatically reduced in thickness along with dystrophic muscle tissue (Figure 7E). Because the oral lesions and laryngeal deformities of $Dsg3^{sqk/sqk}$ mice potentially interfere with solid food uptake, $Dsg3^{sqk/sqk}$ and WT mice were given Ensure Plus shake ad libitum in addition to their regular solid

Figure 5 $Dsg3$ mRNA and protein expression in $Dsg3^{+/+}$ and $Dsg3^{sqk/sqk}$ mice. **A:** $Dsg3^{sqk/sqk}$, $Dsg3^{sqk/+}$, and $Dsg3^{+/+}$ mice express $Dgs3$ transcripts equally. The diagram indicates the positions of the $Dsg3$ cDNA-specific primer pair relative to gene structure. The reverse primer spans the intron between exons 1 and 2 to preclude the amplification of residual genomic DNA after DNAse treatment. The histogram shows real-time quantitative PCR (qPCR) analysis of $Dsg3$ mRNA expression in tongue samples obtained from squeaky (sqk) homozygous ($Dsg3^{sqk/sqk}$, $n = 4$), heterozygous ($Dsg3^{sqk/+}$, $n = 5$), and wild-type (WT; $n = 3$) mice. **B:** Western blot analysis of Dsg3 protein expression by tongue and skin. $Dsg3^{sqk/sqk}$ mice expressed a hypomorphic Dsg3 protein of approximately 110 kDa, whereas $Dsg3^{sqk/+}$ mice expressed both truncated (approximately 110 kDa) and full-length (approximately 125 kDa) Dsg3 proteins. Non-Dsg3 proteins recognized by the anti-Dgs3 polyclonal antibody are indicated as cross-reactive. ERK2 protein was used as a control for equivalent total protein loading between samples. **C:** Altered mechanical integrity of cultured keratinocyte monolayers from $Dsg3^{sqk/sqk}$ and $Dsg3^{sqk/+}$ mice. Cell monolayers were incubated in the presence of 1.2 mmol/L calcium for 72 hours and treated with dispase II before mechanical disruption. The histogram indicates the number of monolayer fragments observed after shaking, with representative cell monolayers shown on the right. **D:** Western blot analysis of Dsg3, desmocollins 1 and 3 (Dsc1 and Dsc3, respectively), and plakoglobin (PG) expression by cultured keratinocytes. ERK2 is shown as a loading control. $*P < 0.05$.
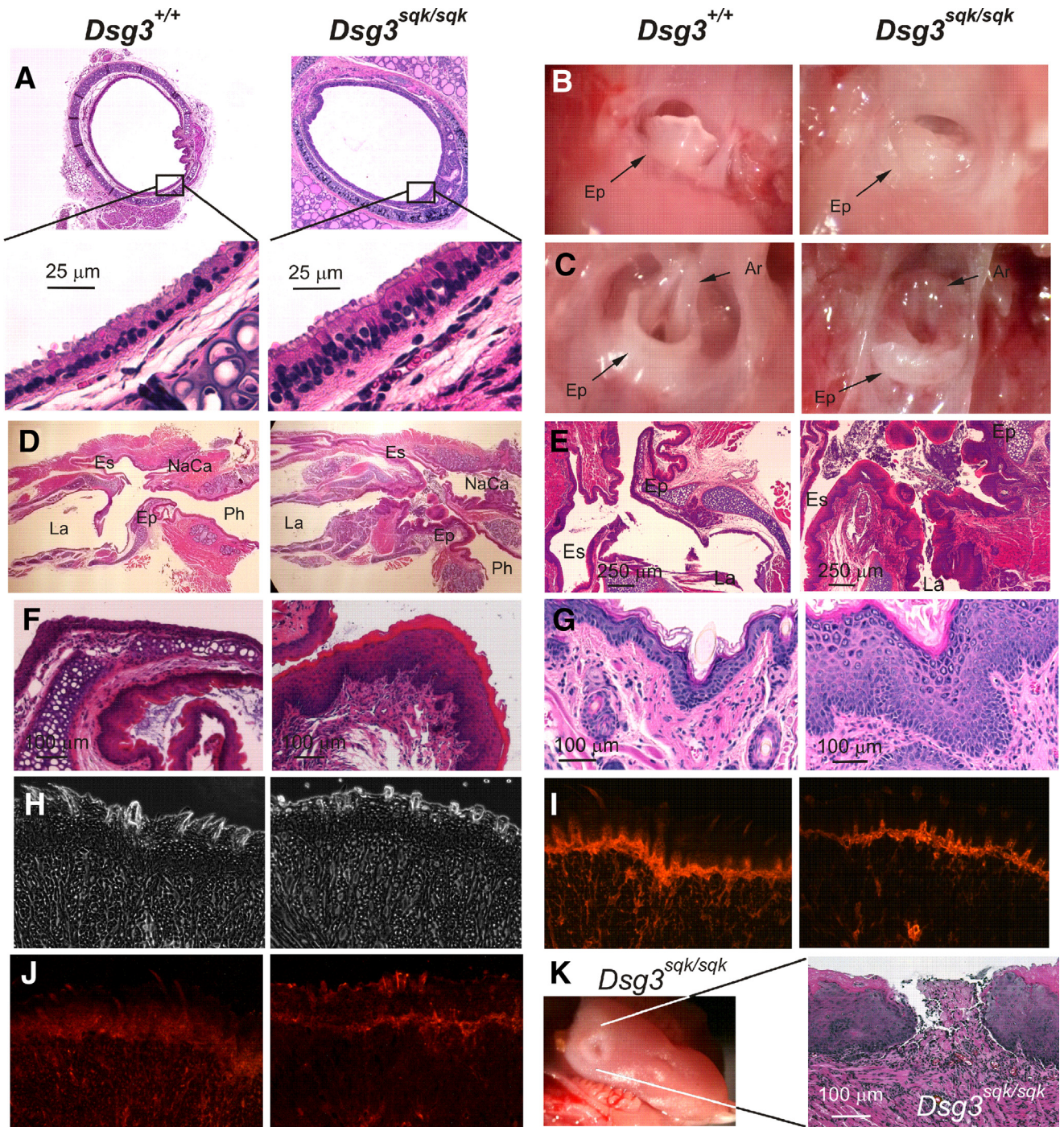
Figure 6 Trachea, snout, and tongue tissue sections from *Dsg3^{sqk/sqk}* and *Dsg3^{+/+}* littermates. **A:** Trachea cross sections obtained from 6-month-old mice of each genotype show a thickening of the pseudostratified ciliated columnar epithelium in *Dsg3^{sqk/sqk}* mice. **B:** Representative views of the epiglottis (Ep) from the mouth. The epiglottis of wild-type (WT) mice is well shaped and pointy, whereas the epiglottis of *Dsg3^{sqk/sqk}* mice is hyperplasic, amorphous, and enlarged. **C:** Representative view of the epiglottis from the top with the tongue pulled forward. Arytenoid ridges (Ar) are clearly visible in the WT littermate mouse. Epiglottis hyperplasia in *Dsg3^{sqk/sqk}* mice results in a narrowed laryngeal opening. **D:** Hematoxylin and eosin (H&E) staining of representative sagittal tissue sections of the larynx. Labels indicate the larynx (La), epiglottis (Ep), pharynx (Ph), esophagus (Es), and nasal cavity (NaCa). **E and F:** Representative higher-magnification images of the upper larynx from **D** show severe hyperplasia of the subglottic epithelium in *Dsg3^{sqk/sqk}* mice. **G:** Representative tissues sections of healthy snout skin from a WT mouse and from a snout skin erosion site of a 9-month-old *Dsg3^{sqk/sqk}* mouse show epidermal thickening of the stratum spinosum. **H and I:** Representative desmoplakin immunofluorescence staining in the tongue of WT mice relative to *Dsg3^{sqk/sqk}* mice. Shown are frozen tongue tissue sections stained with anti-desmoplakin antibody (Ab); brightfield images (**H**) and immunofluorescence images (**I**) taken with the same exposure times. **J:** Representative plakoglobin immunofluorescence staining in the tongue of WT mice relative to *Dsg3^{sqk/sqk}* mice. Shown are frozen tongue tissue sections stained with anti-plakoglobin Ab; immunofluorescence images were taken with the same exposure times. **K:** Image and H&E-stained tissue section of an epithelial lesion on the tongue of a representative 4-week-old *Dsg3^{sqk/sqk}* mouse. **A–K:** Similar results were obtained from tissues of two or more littermates of each genotype.

A

B

C

D

E

100 μm *Dsg3*$^{+/+}$ 100 μm *Dsg3*$^{sqk/sqk}$

F

G
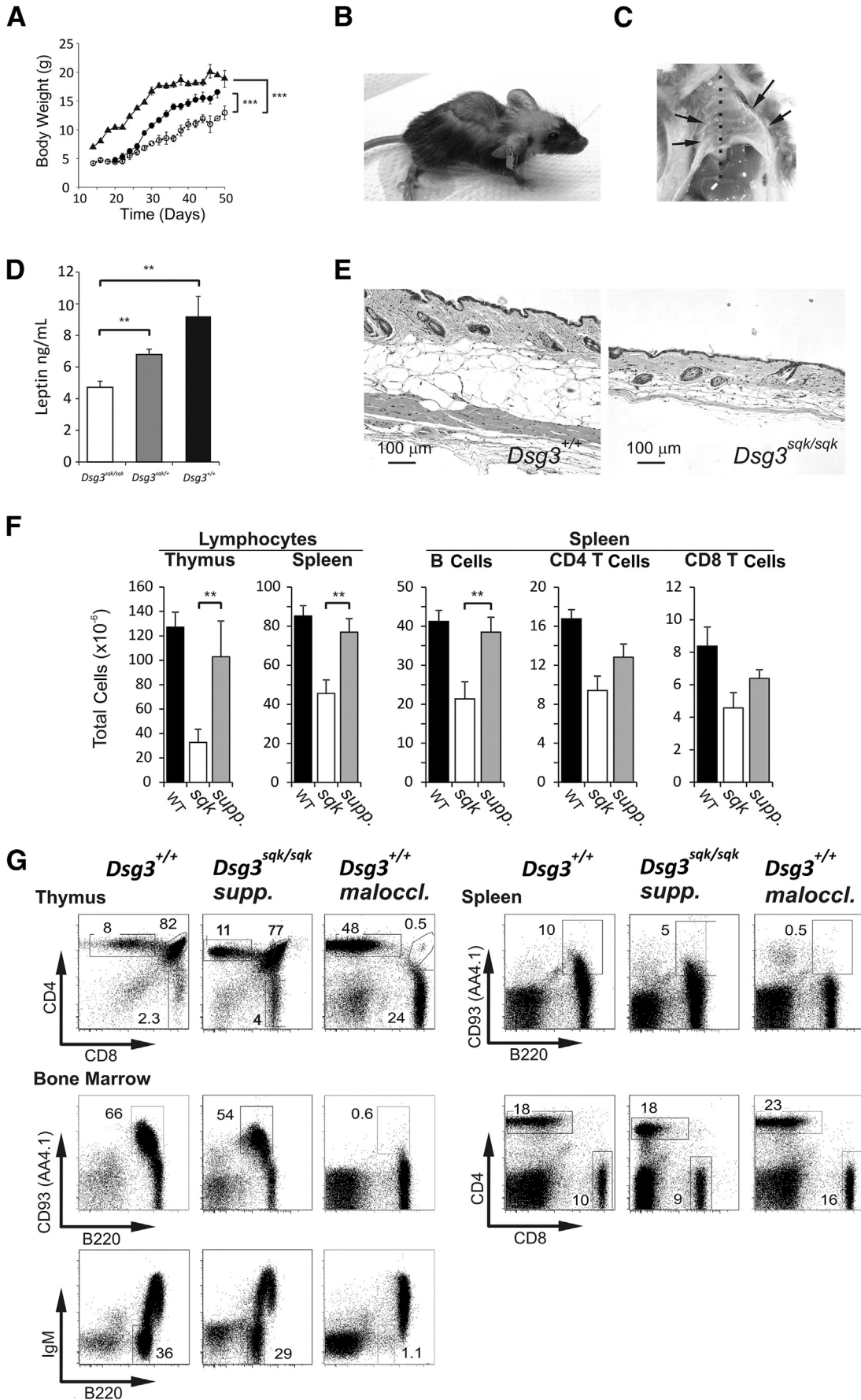
diet. $Dsg3^{sqk/sqk}$ mice on the supplemented diet had 100% survival rates over 49 days, and their body weights increased significantly (Figure 7A). Nutritional supplementation also normalized thymus, bone marrow, and spleen B and T cell numbers and development in $Dsg3^{sqk/sqk}$ mice when compared with $Dsg3^{sqk/sqk}$ mice on solid-food diets (Figure 7, F and G). Ensure Plus supplementation did not increase the mean body weights of WT littermates or alter the cyclic hair loss, inspiratory stridor (squeaking), larynx hyperplasia, and epithelium thickening, but it altered tissue architecture observed in $Dsg3^{sqk/sqk}$ mice (data not shown).

Lymphocyte development was also assessed in three mice that spontaneously developed frontal incisor malocclusions and become runted because of acute malnutrition. Remarkably, thymus, bone marrow, and spleen lymphocyte development in WT mice with malocclusion (Figure 7G) was nearly identical to what was observed in $Dsg3^{sqk/sqk}$ mice of comparable ages (Figures 2 and 7G). Thus, the reduced body weight and acquired immunodeficiency observed in $Dsg3^{sqk/sqk}$ mice are likely to result from inadequate nutrition.

Discussion

Mice with a unique autosomal recessive squeaky phenotype due to hypomorphic Dsg3 protein expression were identified. The hypomorphic Dsg3 protein resulted from an in-frame $Dsg3$ gene deletion that removed 81% (69 amino acids) of the extracellular EC2 domain of the protein. The characteristic squeaking phenotype of $Dsg3^{sqk/sqk}$ mice resulted from airway obstructions and thickened epithelial layers, with characteristic lesions observed on abraded epithelial tissues as the mice aged. As a likely consequence of tissue hypertrophy and lesions, the mice developed a dramatic wasting syndrome starting at 2 weeks of age that resulted in significant runting and reduced body fat deposition. The severe wasting syndrome of $Dsg3^{sqk/sqk}$ mice resulted in acquired immunodeficiency even though Dsg3 expression is not reported within the immune system. Both wasting and immunodeficiency were reversed by supplemental nutrition, demonstrating that the phenotype of $Dsg3^{sqk/sqk}$ mice primarily results from intrinsic genetic

alterations in desmosome assembly within epithelial tissues. Remarkably, the $Dsg3^{sqk/sqk}$ phenotype includes features that are different from what occurs in $Dsg3^{-/-}$ mice that serve as an important animal model for human pemphigus vulgaris.[9]

$Dsg3^{sqk/sqk}$ mice developed tongue lesions, but they did not develop discernable acantholysis in any other examined tissues. $Dsg3^{-/-}$ mice develop widespread skin, mucosal, and vaginal blisters as well as ulcerative lesions resulting from suprabasilar acantholysis.[10] Thereby, hypomorphic Dsg3 protein expression in $Dsg3^{sqk/sqk}$ mice may be sufficient for intercellular adhesion that prevents spontaneous acantholysis, but insufficient to prevent epithelial lesions resulting from mechanical damage or stresses, such as chewing on solid food particles. Multiple other phenotypic features of $Dsg3^{sqk/sqk}$ mice, such as hair and weight loss, appear to be more severe than those observed in $Dsg3^{-/-}$ mice. A distinct histopathological feature of $Dsg3^{sqk/sqk}$ mice was a thickening of airway pseudostratified ciliated epithelium, potentially contributing to airway obstruction and stridor (Figure 6A and Supplemental Video S1). Similarly, hyperplasia of the stratum spinosum was observed in sections of larynx epithelium and snout epidermis from $Dsg3^{sqk/sqk}$ mice. The stratum spinosum is enriched in desmosomal connections between adjacent cells. Most dramatic was the acquired immunodeficiency observed in $Dsg3^{sqk/sqk}$ mice, which is not observed in $Dsg3^{-/-}$, $Dsg3^{bal-2J}$, or $Dsg3^{bal-Pas}$ mice. Transgenic mice expressing a Dsg3 variant lacking the extracellular portion of the protein also demonstrate a phenotype distinct from $Dsg3^{-/-}$ mice, including markedly swollen paws in neonatal mice, epidermal flaking, and progressive necrosis of the tail tip.[24] Desmosomes may also contribute to tissue morphogenesis.[25] In patients with mutations in $Dsg1$ that experience striate palmoplantar keratodermas, hyperkeratosis is frequently observed around lesions and sites of mechanical stress, such as the soles and palms.[26–28] Thereby, hypomorphic Dsg3 protein expression may disrupt desmosome structure and alter cell-cell interactions that are insensitive to total Dsg3 deficiency.

In comparison with $Dsg3^{sqk/sqk}$ mice, $Dsg3^{-/-}$ mice exhibit a less pronounced, but similar, pattern of cyclical hair

Figure 7 $Dsg3^{sqk/sqk}$ and malnourished wild-type (WT) mice share similar phenotypes. **A:** $Dsg3^{sqk/sqk}$ mice on solid-food diets have reduced body weights, but gain weight when the diet is supplemented with Ensure Plus starting at birth. Weights of WT (black triangles), $Dsg3^{sqk/sqk}$ (white circles), and Ensure Plus fed $Dsg3^{sqk/sqk}$ (black circles) littermates were compared among 10- to 49-day-old animals. Bars indicate SE; significance was determined by analysis of covariance. A total of 4 to 14 mice were used per data point. **B:** The emaciated appearance of a representative 3-month-old $Dsg3^{sqk/sqk}$ mouse. **C:** Rib cage deformity was observed in approximately 2% of $Dsg3^{sqk/sqk}$ mice. The dotted line indicates the sternum, and **arrows** indicate deviations of cage shape. **D:** Serum leptin levels of $Dsg3^{sqk/sqk}$ mice were determined by enzyme-linked immunosorbent assay. $n = 6$, $Dsg3^{sqk/sqk}$; $n = 4$, $Dsg3^{sqk/+}$; $n = 5$, WT. **E:** Representative reduced s.c. fat deposits and muscle mass in $Dsg3^{sqk/sqk}$ mice. The images show cross sections of skin from the backs of 9-month-old WT and $Dsg3^{sqk/sqk}$ littermates that are representative of three littermate pairs. **F:** Nutrient supplementation (supp.) results in a significant increase of mean thymocyte, splenocyte, and spleen B-cell numbers in four $Dsg3^{sqk/sqk}$ mice. **G:** Effects of nutritional deficiency on T- and B-lymphocyte development. Thymus, bone marrow, and spleen obtained from 6-week-old littermates without ($Dsg3^{+/+}$) malocclusion, with spontaneous frontal incisor malocclusion ($Dsg3^{+/+}$ maloccl.), or $Dsg3^{sqk/sqk}$ mice on Ensure Plus—supplemented diet ($Dsg3^{sqk/sqk}$ supp.) were analyzed by immunofluorescence staining. Numbers indicate representative percentages of cells within the indicated gates. The gates define double-positive (CD4$^+$CD8$^+$) and single-positive (CD4$^-$CD8$^+$ or CD4$^+$CD8$^-$) thymocytes; pre- and immature (CD93$^+$B220^{low}) B cells and pre-B (B220^{low}IgM$^-$) cells in bone marrow, transitional B cells (CD93$^+$B220$^+$), and T-cell subsets. Three mice with malocclusion and four mice on supplemented diet were analyzed. **$P < 0.01$, ***$P < 0.001$.

loss and regrowth beginning at a young age. *Dsg3* is highly expressed by skin keratinocytes that surround hair shafts. *Dsg3* ablation in *Dsg3*$^{-/-}$ mice reduces interactions between the basal layer of the outer root sheath epithelium and the cells surrounding a hair club, resulting in weak anchoring of the hair shaft and its loss during the telogen growth phase. Delayed growth of new hairs also exacerbates the balding appearance in *Dsg3*$^{-/-}$ mice.[11] Although a cyclical hair loss pattern does not occur in pemphigus patients, alopecia is observed frequently.[29] Dsg3 and Dsc3 heterodimerize in the basal layers of the epidermis.[30] Similar to *Dsg3*$^{-/-}$ mice, conditional deletion of *Dsc3* in the skin causes a cyclical hair loss pattern resulting from defects during the telogen phase.[31] Mutations in other desmosomal cadherins also affect hair growth. Reduced or absent hair growth in human hereditary recessive hypotrichosis maps to the *Dsg4* locus.[32–34] However, *Dsg4*-deficient mice develop alopecia due to breakage of their brittle hairs.[35] Hair loss in mice deficient for *Dsc1* is associated with skin ulcerations.[1] *Dsg3*$^{bal-2J}$ and *Dsg3*$^{bal-Pas}$ mice also demonstrate balding, reduced body fat deposits, tongue ulcerations, inflammatory lesions of the eyelids, and blisters/ulcerations of the footpads due to an absence of Dsg3 protein expression.[10,12,13,23] The *Dsg3*$^{bal-2J}$ mutation results from a single-nucleotide insertion that prematurely terminates translation.[10] The *Dsg3*$^{bal-Pas}$ mutation results from a 14-bp deletion that leads to translation termination.[23] Thereby, *Dsg3*$^{sqk/sqk}$ mice represent a spontaneous mutation in the *Dsg3* gene that leads to the expression of a novel splice-variant protein and results in a unique mouse phenotype.

The individual cadherin domains of the desmosomal protein families (eg, EC1 to EC4 of Dsg3) are highly organized structurally and adopt a stable, curved conformation that is required for associations between the N-terminal EC1 domain in both *trans-* or *cis-* configurations with the EC1 domains of other cadherins.[36] The extracellular cadherin domains are critical for optimizing spatial orientations and the formation of zipper-like desmosomal junctions between cells that are required for optimal intercellular adhesion and tissue integrity.[36] The truncation of the EC2 domain in *Dsg3*$^{sqk/sqk}$ mice likely perturbs the formation of tightly packed desmosomes. Consistently, Dsg3^{sqk} and Dsc3 protein expression levels were reduced in newborn skin keratinocytes, whereas Dsc1 and plakoglobin expression levels were unaffected (Figure 5D). However, desmoplakin and plakoglobin were reduced within adult tongue tissues of *Dsg3*$^{sqk/sqk}$ mice (Figure 6, H–J). Other desmosome constituents may also be altered within tissues of *Dsg3*$^{sqk/sqk}$ mice. The polyclonal antibody used to identify mouse Dsg3 cross-reacted with other proteins of higher molecular mass, one of which was enriched in *Dsg3*$^{sqk/sqk}$ tongue (Figure 5B). On the basis of predicted molecular weights, the cross-reactive band(s) may be Dsg1, which is highly expressed and 44% identical in amino acid sequence with Dsg3, or may be Dsc2, which is expressed at 10-fold higher levels in tongue relative to skin and which shares 32% amino acid sequence identity with Dsg3 (Gene Skyline, *http://www.immgen.org/databrowser/*

index.html, last accessed October 23, 2014). Disruption in the ordered molecular complexes where Dsg3 is normally highly expressed may result in weakened epithelial layers that enable modest mechanical stresses to cause abnormal levels of damage, leading to skin and mucosal surface ulcerations. Indeed, mechanical stress resistance was reduced in cells from *Dsg3*$^{sqk/sqk}$ mice (Figure 5C). Thereby, alterations in Dsg3 protein structure may induce pathological changes that disrupt normal cadherin function and reduce desmosome densities beyond what is observed in *Dsg3*$^{-/-}$ mice.

Dsg3$^{sqk/sqk}$ and WT littermates were visually indistinguishable during the first and second weeks after birth, with detectable size differences by days 10 to 14. Laryngeal deformities and accompanying malnutrition became severe in *Dsg3*$^{sqk/sqk}$ mice as early as 3 weeks of age when most pups begin to supplement dam milk with solid food, which led to an accompanying wasting disease and reduced numbers of B- and T-lineage cells in the bone marrow and spleen (Figures 2 and 6). Obstructions within the pharynx probably limit food intake in *Dsg3*$^{sqk/sqk}$ mice, leading to a malnutrition phenotype. Lesions in the oral mucosa are also postulated to reduce food consumption in *Dsg3*$^{-/-}$ mice,[10] although these mice maintain normal immune systems. Malnutrition is a well-known cause of immunodeficiency, affecting the immune system through multiple mechanisms. Malnutrition changes the bone marrow stromal microenvironment, impairs hematopoiesis, and leads to thymic atrophy due to immature CD4/CD8 double-positive thymocyte apoptosis.[37,38] Consistently, starving mice with frontal incisor malocclusions had an immune phenotype similar to *Dsg3*$^{sqk/sqk}$ mice (Figure 7G). Significantly reduced leptin levels were observed in *Dsg3*$^{sqk/sqk}$ mice (Figure 7D), which would contribute to defective hematopoiesis and immune dysfunction.[39,40] Even short-term fasting for as little as 48 hours reduces pre–B- and immature B-cell numbers in the bone marrow.[41] Reduced lymphocyte numbers in malnourished *Dsg3*$^{sqk/sqk}$ mice may render them even more susceptible to infections and explain their accelerated mortality. Remarkably, liquid diet supplementation reversed wasting in *Dsg3*$^{sqk/sqk}$ mice and normalized their survival rates as well as pre–B- and immature B-cell numbers in both the spleen and bone marrow, but it did not reduce hyperplasia of the epiglottis (Figure 6). More important, nutritional supplementation specifically affected *Dsg3*$^{sqk/sqk}$ mice because only normal weight gains were observed in control WT littermates. Thus, the acquired immunodeficiency of *Dsg3*$^{sqk/sqk}$ mice is secondary to malnutrition.

In conclusion, this study characterizes a spontaneous recessive mutation in the *Dsg3* gene that uniquely results in the expression of a hypomorphic Dsg3 protein that confers a striking and distinct phenotype. Remarkably, the *Dsg3*$^{sqk/sqk}$ mutation does not result in the hallmark skin blisters and acantholysis found in *Dsg3*$^{-/-}$ mice, although expression of this E2 domain–deficient Dsg3 variant leads to a more severe phenotype, including wasting disease. *Dsg3*$^{sqk/sqk}$ mice thereby offer new insights into the complex nature of how desmosomal

cadherins orchestrate tissue integrity and general health. There is, therefore, a potential for genetic alterations similar to those in $Dsg3^{sqk/sqk}$ mice to induce human disease, whereas the characteristic blisters of pemphigus may not be present.

Acknowledgments

Supplemental Data

Supplemental material for this article can be found at http://dx.doi.org/10.1016/j.ajpath.2014.10.025.

References

1. Holthofer B, Windoffer R, Troyanovsky S, Leube RE: Structure and function of desmosomes. Int Rev Cytol 2007, 264:65−163
2. Garrod DR, Merritt AJ, Nie Z: Desmosomal cadherins. Curr Opin Cell Biol 2002, 14:537−545
3. Heng TS, Painter MW: The Immunological Genome Project: networks of gene expression in immune cells. Nat Immunol 2008, 9:1091−1094
4. Hulpiau P, van Roy F: Molecular evolution of the cadherin super-family. Int J Biochem Cell Biol 2009, 41:349−369
5. Dusek RL, Godsel LM, Green KJ: Discriminating roles of desmosomal cadherins: beyond desmosomal adhesion. J Dermatol Sci 2007, 45:7−21
6. Amagai M, Matsuyoshi N, Wang ZH, Andl C, Stanley JR: Toxin in bullous impetigo and staphylococcal scalded-skin syndrome targets desmoglein 1. Nat Med 2000, 6:1275−1277
7. Eshkind L, Tian Q, Schmidt A, Franke WW, Windoffer R, Leube RE: Loss of desmoglein 2 suggests essential functions for early embryonic development and proliferation of embryonal stem cells. Eur J Cell Biol 2002, 81:592−598
8. Den Z, Cheng X, Merched-Sauvage M, Koch PJ: Desmocollin 3 is required for pre-implantation development of the mouse embryo. J Cell Sci 2006, 119:482−489
9. Amagai M: Pemphigus vulgaris and its active disease mouse model. Curr Dir Autoimmun 2008, 10:167−181
10. Koch PJ, Mahoney MG, Ishikawa H, Pulkkinen L, Uitto J, Shultz L, Murphy GF, Whitaker-Menezes D, Stanley JR: Targeted disruption of the pemphigus vulgaris antigen (desmoglein 3) gene in mice causes loss of keratinocyte cell adhesion with a phenotype similar to pemphigus vulgaris. J Cell Biol 1997, 137:1091−1102
11. Koch PJ, Mahoney MG, Cotsarelis G, Rothenberger K, Lavker RM, Stanley JR: Desmoglein 3 anchors telogen hair in the follicle. J Cell Sci 1998, 111:2529−2537
12. Davisson MT, Cook SA, Johnson KR, Eicher EM: Balding: a new mutation on mouse chromosome 18 causing hair loss and immuno-logical defects. J Hered 1994, 85:134−136
13. Montagutelli X, Lalouette A, Boulouis HJ, Guenet JL, Sundberg JP: Vesicle formation and follicular root sheath separation in mice ho-mozygous for deleterious alleles at the balding (bal) locus. J Invest Dermatol 1997, 109:324−328
14. Zhou L-J, Smith HM, Waldschmidt TJ, Schwarting R, Daley J, Tedder TF: Tissue-specific expression of the human CD19 gene in

15. Pfaffl MW: A new mathematical model for relative quantification in real-time RT-PCR. Nucleic Acids Res 2001, 29:e45
16. Zhou K, Muroyama A, Underwood J, Leylek R, Ray S, Soderling SH, Lechler T: Actin-related protein2/3 complex regulates tight junctions and terminal differentiation to promote epidermal barrier formation. Proc Natl Acad Sci U S A 2013, 110:E3820−E3829
17. Kountikov E, Nayak D, Wilson M, Miller NW, Bengten E: Expression of alternatively spliced CD45 isoforms by channel catfish clonal T and B cells is dependent on activation state of the cell and regulated by protein synthesis and degradation. Dev Comp Immunol 2004, 34:1109−1118
18. Caldelari R, Suter MM, Baumann D, De Bruin A, Muller E: Long-term culture of murine epidermal keratinocytes. J Invest Dermatol 2000, 114:1064−1065
19. Huen AC, Park JK, Godsel LM, Chen X, Bannon LJ, Amargo EV, Hudson TY, Mongiu AK, Leigh IM, Kelsell DP, Gumbiner BM, Green KJ: Intermediate filament-membrane attachments function synergistically with actin-dependent contacts to regulate intercellular adhesive strength. J Cell Biol 2002, 159:1005−1017
20. Simpson CL, Kojima S, Cooper-Whitehair V, Getsios S, Green KJ: Plakoglobin rescues adhesive defects induced by ectodomain truncation of the desmosomal cadherin desmoglein 1: implications for exfoliative toxin-mediated skin blistering. Am J Pathol 2010, 177:2921−2937
21. Drake JW, Charlesworth B, Charlesworth D, Crow JF: Rates of spontaneous mutation. Genetics 1998, 148:1667−1686
22. Kumar S, Subramanian S: Mutation rates in mammalian genomes. Proc Natl Acad Sci U S A 2002, 99:803−808
23. Pulkkinen L, Choi YW, Simpson A, Montagutelli X, Sundberg J, Uitto J, Mahoney MG: Loss of cell adhesion in Dsg3bal-Pas mice with homozygous deletion mutation (2079del14) in the desmoglein 3 gene. J Invest Dermatol 2002, 119:1237−1243
24. Allen E, Yu QC, Fuchs E: Mice expressing a mutant desmosomal cadherin exhibit abnormalities in desmosomes, proliferation, and epidermal differentiation. J Cell Biol 1996, 133:1367−1382
25. Lai-Cheong JE, Arita K, McGrath JA: Genetic diseases of junctions. J Invest Dermatol 2007, 127:2713−2725
26. Dua-Awereh MB, Shimomura Y, Kraemer L, Wajid M, Christiano AM: Mutations in the desmoglein 1 gene in five Pakistani families with striate palmoplantar keratoderma. J Dermatol Sci 2009, 53:192−197
27. Barber AG, Wajid M, Columbo M, Lubetkin J, Christiano AM: Striate palmoplantar keratoderma resulting from a frameshift mutation in the desmoglein 1 gene. J Dermatol Sci 2007, 45:161−166
28. Zamiri M, Smith FJ, Campbell LE, Tetley L, Eady RA, Hodgins MB, McLean WH, Munro CS: Mutation in DSG1 causing autosomal dominant striate palmoplantar keratoderma. Br J Dermatol 2009, 161:692−694
29. Veraitch O, Ohyama M, Yamagami J, Amagai M: Alopecia as a rare but distinct manifestation of pemphigus vulgaris. J Eur Acad Dermatol Venereol 2013, 27:86−91
30. Spindler V, Heupel WM, Efthymiadis A, Schmidt E, Eming R, Rankl C, Hinterdorfer P, Muller T, Drenckhahn D, Waschke J: Des-mocollin 3-mediated binding is crucial for keratinocyte cohesion and is impaired in pemphigus. J Biol Chem 2009, 284:30556−30564
31. Chen J, Den Z, Koch PJ: Loss of desmocollin 3 in mice leads to epidermal blistering. J Cell Sci 2008, 121:2844−2849
32. Rafique MA, Ansar M, Jamal SM, Malik S, Sohail M, Faiyaz-Ul-Haque M, Haque S, Leal SM, Ahmad W: A locus for hereditary hypotrichosis localized to human chromosome 18q21.1. Eur J Hum Genet 2003, 11:623−628
33. Shimomura Y, Sakamoto F, Kariya N, Matsunaga K, Ito M: Mutations in the desmoglein 4 gene are associated with monilethrix-like congenital hypotrichosis. J Invest Dermatol 2006, 126:1281−1285
34. Wajid M, Bazzi H, Rockey J, Lubetkin J, Zlotogorski A, Christiano AM: Localized autosomal recessive hypotrichosis due to a frameshift

mutation in the desmoglein 4 gene exhibits extensive phenotypic variability within a Pakistani family. J Invest Dermatol 2007, 127: 1779−1782

35. Kljuic A, Bazzi H, Sundberg JP, Martinez-Mir A, O'Shaughnessy R, Mahoney MG, Levy M, Montagutelli X, Ahmad W, Aita VM, Gordon D, Uitto J, Whiting D, Ott J, Fischer S, Gilliam TC, Jahoda CA, Morris RJ, Panteleyev AA, Nguyen VT, Christiano AM: Desmoglein 4 in hair follicle differentiation and epidermal adhesion: evidence from inherited hypotrichosis and acquired pemphigus vulgaris. Cell 2003, 113:249−260

36. Al-Jassar C, Bikker H, Overduin M, Chidgey M: Mechanistic basis of desmosome-targeted diseases. J Mol Biol 2013, 425:4006−4022

37. Xavier JG, Favero ME, Vinolo MA, Rogero MM, Dagli ML, Arana-Chavez VE, Borojevic R, Borelli P: Protein-energy malnutrition alters histological and ultrastructural characteristics of the bone marrow and decreases haematopoiesis in adult mice. Histol Histopathol 2007, 22: 651−660

38. Savino W, Dardenne M: Nutritional imbalances and infections affect the thymus: consequences on T-cell-mediated immune responses. Proc Nutr Soc 2010, 69:636−643

39. Saucillo DC, Gerriets VA, Sheng J, Rathmell JC, Maciver NJ: Leptin metabolically licenses T cells for activation to link nutrition and immunity. J Immunol 2014, 192:136−144

40. Claycombe K, King LE, Fraker PJ: A role for leptin in sustaining lymphopoiesis and myelopoiesis. Proc Natl Acad Sci U S A 2008, 105: 2017−2021

41. Tanaka M, Suganami T, Kim-Saijo M, Toda C, Tsuiji M, Ochi K, Kamei Y, Minokoshi Y, Ogawa Y: Role of central leptin signaling in the starvation-induced alteration of B-cell development. J Neurosci 2011, 31:8373−8380